Contents lists available at ScienceDirect

Fuel Processing Technology

journal homepage: www.elsevier.com/locate/fuproc





Experimental investigation performance and emission of hydrotreated pyrolysis oil in a heavy-duty engine with EGR

Jinlin Han a,c,*, L.M.T. Somers a, Bert van de Beld b

- a Department of Mechanical Engineering, Eindhoven University of Technology, Netherlands
- ^b BTG Biomass Technology Group BV, Netherlands
- ^c TNO Automotive, Helmond, Netherlands

ARTICLE INFO

Keywords: Biofuel PM NOx

EGR

Engine

ABSTRACT

Drop-in biofuels can play an important role in the transition from fossil-based fuels to carbon-neutral energy carriers. This work focuses on performance and emission of hydrotreated pyrolysis oil (HPO) for heavy-duty (HD) engines application. The HPO is blended with marine gas oil (MGO) in various mass ratios and tested both in combustion research unit (CRU) and engine facilities. Typical cruise speeds and multiple loads are selected in the heavy-duty engine tests. Both inlet temperature and EGR rate are varied to investigate the effects of control parameters on HPO. The results reveal that HPO present lower reactivity than MGO and diesel under CRU condition. It can function as a drop-in fuel without any modification to the engine and no recalibration was required. Specifically, key combustion phases are noticed to be identical. The engine can run smoothly and safely at 50% blend ratio with 1% reduction on net indicated efficiency (NIE) and 0.002 g/kWh particulate matter emissions (PM). At low load, the NOx emissions decrease to 1 g/kWh at 40% EGR, yet 1% decrease of NIE is shown. While all fuels yield more NOx but less PM emissions as the increase of inlet temperature. Inlet heating does decrease the NIE by 1%.

1. Introduction

Nowadays, about 23% of global CO2 emissions are generated from the transportation sector, and it is still growing globally [1]. Problems associated with the use of fossil fuels such as climate change and energy security have risen significant concerns. It sparked a renewed interest in reducing the usage of fossil-based fuels and advocating de-carbonization. The transition from petroleum to a fully new non-carbon energy carrier is by no means an overnight exercise and requires decades of effort to create the necessary infrastructure. Hence, there is a growing interest in applying drop-in biofuels in existing engine facilities either as component fuels or alternative fuels. The advantage of applying drop-in biofuels lies in the closed CO₂ life cycle and reusing the existing storage, transportation, and distribution facilities. The ability to combine biofuels with advanced engine technologies without jeopardizing the engine hardware is crucial for the implementation of these fuels.

The study for clean alternative fuels has been developing and its specifications are driven by the engine technology, existing fossil fuel specification, and availability of feedstock in a specific geographic location. Among all the techniques applying biofuel in engines, such as port fuel injection, fumigation, and drop-in component or completely as a self-sustained alternative fuel, drop-in or splash blend with commercial fuels is the most feasible application due to the ease of operation and its low cost [2].

There are a few candidates researched and studied intensively in the literature. For example, 2,5-dimethylfuran (DMF), which is one of the biofuels considered to be quite promising, could be produced on a commercial scale through high-efficiency catalyst reactions [3].

Abbreviations: aTDC, After top dead center; BD, Burn duration; B7, Diesel contains 7% bio-component; CA, Crank angle; CN, Cetane Number; CR, Compression ratio; DMF, 2,5-dimethylfuran; DNBE, di-n-butylether; DI, Direction injection; 2-EHN, 2-ethylhexyl nitrate; EGR, Exhaust gas recirculation; EOC, End of combustion; EOI, End of injection; EU, European union; FPBO, Fast pyrolysis bio-oil; FSN, Filtered smoke number; HD, Heavy-duty; HPO, Hydro-treated pyrolysis oil; HVO, Hydro-treated vegetable oil; ISCO, Indicated specific carbon monoxide; ID, Ignition delay; ISNOx, Indicated specific nitro-oxide; ISTHC, Indicated specific unburnt hydrocarbon; LRF, Low reactivity fuel; nIMEP, Net indicated mean effective pressure; MGO, Marine gas oil; NOx, Nitrogen oxides; PM, Particulate matters; PRR, Pressure rise rate; RCCI, Reactivity controlled compression ignition; RPM, Rotation per minute; SPO, Stabilized pyrolysis oil.

Corresponding author at: Department of Mechanical Engineering, Eindhoven University of Technology, Netherlands. E-mail address: j.han.1@tue.nl (J. Han).

Possessing similar physicochemical properties to fossil fuels, DMF was reported to be an ideal drop-in fuel in diesel, leading to lower combustion temperature and longer ignition delay (ID) due to higher latent heat of vaporization. To match the combustion phasing, 2-Ethylhexyl nitrate (2-EHN) was used to decrease the ID of DMF/Diesel blends in the compression ignition (CI) engine. And EGR was found to increase the ID of DMF/Diesel blends and therefore higher pressure rise rate [4]. As the load increased, the ID differences were smaller regardless of the blend ratio (D10, D20, D30, D40, and diesel fuel). The longer ID at low load conditions was assumed either due to the lower cetane number (CN) of DMF or lower equivalence ratio [5]. And increasing the engine speed was shown to increase the ID as well [6]. The burn duration (BD) of DMF/Diesel blends was shorter than that of diesel and biodiesel due to increased mixing time and more premixed combustion fraction. Consequently, the combustion duration decreases as the DMF blend ratio increases [7]. Like diesel and biodiesel, the ID of DMF fuel blends shortens as the injection timing retards [8]. And DMF blend ratio was noticed to be limited by the extremely high peak pressure, pressure rise rate (PRR), engine noise, and therefore higher mechanical loads on the engine bulk [9]. Soot reduction was attributed as the most beneficial trait as an alternative fuel in CI engines. Up to 90% decrease in engine-out soot emission was shown at a 40% DMF blend ratio compared with regular diesel. This is assumed due to longer ID, high volatility, and more premixed combustion. Nevertheless, the NOx emissions were observed to be 40% higher than that of diesel when operated without EGR [6].

Other promising biofuel candidates are alcoholic fuels, which are considered typical biofuel types appropriate to engines and some of them have been produced on the industrial and commercial scale [10]. The oxygenated fuel structure on the one hand contributes to low soot emissions, on the other decreases the energy density [11]. As the carbon number and chain increase, both the fuel reactivity and energy density increase [12]. Short-chain alcohols (methanol, ethanol, and propanol) show extremely low reactivity and are suitable for spark ignition and low-temperature combustion concepts [13]. When blended with commercial fuels, ethanol, and butanol generally suffer from high peak and cylinder pressure and limited operating range [14,15]. Yet, the low reactivity of ethanol and butanol are perfect candidates for the low reactivity fuel (LRF) in Dual-fuel combustion [16] and RCCI [17,18].

The long-chain alcohols (C7-C8) have a higher CN and energy density [19] and are therefore potential renewable component fuels to be blended with commercial fossil fuels for use in diesel engines. Yesilyurt et al. [20] thoroughly investigated the performance and emission characteristics of 1-heptanol in a single-cylinder diesel engine. 1-heptanol (20%)/diesel, biodiesel (20%)/diesel, and 1-heptanol (20%)/biodiesel (20%)/diesel (60%) were splash blended and tested under a wide range (25/50/75/100%) of engine loads at 1500 rpm. At 100% load, the addition of biodiesel and 1-heptanol decreased brake thermal efficiency and peak heat release. And 1-heptanol fuel blends show less CO and HC emissions but higher NOx emissions compared to diesel. The comparison of n-butanol, isobutanol, 2-ethyl hexanol, and n-octanol functions as drop-in fuels with diesel was illustrated in [21,22], where all the blends were applied in existing engines with factory settings. The fuel blends are designed in a certain composition and blend ratio to achieve an overall CN similar to diesel. To reach that objective, hydro-treated vegetable oil (HVO) was added to the blends to compensate for the low reactivity of the alcohols. The combustion process and thermal efficiencies of the designed fuel blends resemble that of conventional diesel combustion. Yet, the alcohol/diesel produced about 50% less soot. Life-cycle analysis shows that 22% to 58% greenhouse gas reduction can be achieved for these specific alcohol/diesel blends compared to pure diesel. The octanol/diesel shows physical properties closer to diesel than butanol/diesel blends. Moreover, cycle-to-cycle variations were observed to be lower, but NOx emissions increased compared to diesel operation [23]. Marius et al. from RWTH [24] compared HVO and noctanol both as self-sustained fuel and drop-in fuels in a diesel engine with default calibration. Pure HVO benefits from a reduction of HC/CO

emissions and combustion noises without sacrificing NOx emissions. HVO yields much lower soot emissions at high loads because of aromatic-free and paraffinic combustion. Due to high CN, HVO leads to slightly higher soot emissions at low load cases, because soot precursors initiate under fuel-rich conditions. Though n-octanol presents the highest combustion noise among tested fuels, no soot emissions were detected from n-octanol. In addition, HC/CO emissions of n-octanol were also noticed to be lower than that of diesel at low loads, while CO emissions were higher than that of diesel at high load conditions. Interestingly, the HVO/1-octanol blends combined the merits of both fuels and eliminate the individual drawbacks. The aforementioned higher soot of HVO fuel at low loads was reduced by more than 50% under operating conditions. This is explained by the oxygen content of noctanol and the lower reactivity of n-octanol. Besides, HC/CO emissions of fuel blends were half of that of diesel without compromising the noise level (3 dB less than low-load diesel operation). The researchers from RWTH and FEV further optimize engine optimization via the design of experiments [25]. More than 1% indicated efficiency gain can be achieved at 14.8 bar indicated mean effective pressure (IMEP) compared to that of diesel. And the aforementioned low soot emissions from HVO and n-octanol fuel could be further halved compared to the baseline calibration. Heuser et al. [26] further studied the influence of fuel structure on exhaust gases of CI engines. Octanol and di-n-butyl ether (DNBE) were selected and compared. Both have identical carbon, oxygen, and hydrogen atom numbers yet have different molecular structures. Both of them can be produced from lignocellulose via a selective chemical transformation process. The engine tests revealed that octanol can completely avoid soot emission while yielding 20% higher HC/CO emissions compared to diesel at part load. This is assumed because of its longer ID (CN \sim 40). DNBE has a CN of 100, but at high load, the combustion is almost soot free with a Euro 6 NOx level before the catalyst. In addition, the over-leaning issue, often observed at low load with fuels having a low reactivity, for octanol is circumvented with DNBE due to its high reactivity.

The aforementioned studies shed light on the attractive properties of drop-in fuels in compression ignition engines. Admittedly, the choice of certain biofuels is dependent on geographic locations, and the specific source should also be renewable. More importantly, the biofuel yield should be high enough for commercial scale, production cost, and scalability should be good as well. There are multiple methods developed to produce advanced biofuels from biomass. This work focuses on fast pyrolysis and its corresponding biofuel. The feedstock is firstly thermal cracked into fast pyrolysis biomass oil (FPBO) and stabilized at a relatively low temperature and high pressure in a hydrogen atmosphere via catalysts. The purpose of the stabilization is to convert the highly reactive functional groups in FPBO such as carbonyls (aldehydes, carbohydrates, ketones). This ends up with the Stabilized Pyrolysis Oil (SPO), which can be further upgraded with commercial hydro-treating catalysts. This hydro-treating process yields the so-called Hydrotreated Pyrolysis Oil (HPO), the specific properties of which can be adjusted by the catalyst applied and the severity of the treatment. For this purpose, NiMo or CoMo catalysts can be selected and further refining could also be performed by applying noble metal catalysts such as Ru/C and Pt/C at elevated conditions. Finally, the HPO may need some after-treatment to obtain suitable drop-in characteristics for marine fuel, e.g., remove lights to increase the flashpoint or remove solid residues by filtration. The final product of HPO must show excellent miscibility with commercial fossil fuels and biofuels in various blend ratios. This work intends to study the application of HPO in marine power generation. Therefore, HPO is blended with marine gas oil (MGO) at a mass ratio of 10%, 30%, and 50%. Pure diesel (contains 7% bio-component, B7) and MGO (free of bio-components) are also tested as reference fuels. The objective of this work is to investigate the working load range for high blend ratio HPO on an HD diesel engine under factory settings with EGR conditions. The resulting engine performance and emission traits of HPO will also be comprehensively illustrated and compared to commercial

fuels (diesel and MGO). And the effects of charge preparation parameters such as EGR rate and inlet temperatures on HPO blends will be intensively discussed.

2. Methodology

First, the combustion research unit (CRU) and engine setup used in this study are briefly introduced (Section 2.1). Then the fuel blends (Section 2.2), the test procedure (Section 2.3), and finally the data analysis method is described (Section 2.4).

2.1. Combustion research unit (CRU) and Engine setup

The investigation starts with investigating the combustion properties of HPO in a constant volume combustion chamber, namely CRU under EGR conditions. A detailed description of this device and operating theory can be found in [27]. The ignition delay of CRU is referred to the time when 0.2 bar pressure increase (start of combustion) is captured after injection timing while burn duration is defined as the time from 0.2 bar pressure increase to 95% maximum pressure increase. The EGR rate of CRU is defined as the pressure ratio of external air and nitrogen supplied to the combustion chamber. During the test, the chamber temperature is fixed at 700 $^{\circ}\text{C}$ to resemble engine cylinder condition after compression while the pressure is varied as 30/40/50 bar. Meanwhile, EGR rate is increased from 0% to 40% in steps of 10% at each chamber pressure case.

Following the tests on CRU, a single-cylinder research engine setup modified from a commercially available 6-cylinder water-cooled 12 L heavy-duty engine is used. Only the first cylinder is firing, using direct injection of tested fuels. The other 5 cylinders are disabled. The specification of the test cylinder is shown in Table 1. The engine is connected to an electrical motor, such that both the speed and load can be controlled. As is shown in Fig. 1, the inlet air is supplied by the external compressed air up to 8 bar. Part of exhaust gases can be redirected, cooled, mixed with fresh air, and charged into the cylinder. Therefore, EGR in this work is referring to dry EGR and is measured by evaluating the CO2 concentration ratio between the inlet and exhaust. The temperature of inlet air is controlled by an electrical heater to maintain the desired inlet temperature. Though both port injection and direct injection (DI) are available for this setup, port injection is not used in this work. Fuel pressure is boosted by the engine fuel pump, distributed by the common rail, and then fed into a Delphi direct injection (DFI21) injector. The setup is equipped with a variety of temperature, pressure, and flow mass sensors for the detection of specific properties of the inlet, exhaust, lubricating oil, cooling water, and fuel flow. The gaseous emissions like unburnt HC, CO, CO2, and NOx are measured by Horiba Mexa-7100DEGR. The soot emissions and particulate matter (PM) are measured by the AVL 451S smoke meter in filtered smoke number (FSN) and converted into weight by Eq. (1) [28].

Table 1 Engine specifications.

Stroke	158 mm
Bore	130 mm
Displacement	2.15 L
Connecting Rod	266.7 mm
Compression ratio	17.2:1
Number of Valves	4
Cylinder head	Low swirl
Piston shape	Double step
Exhaust valve close (EVC)	-359°CA
Intake valve close (IVC)	-174°CA
Exhaust valve open (EVO)	146°CA
Intake valve open (IVO)	357°CA

2.2. Tested fuels and method

In this work, the HPO samples are supplied by BTG [29]. It is firstly produced from the fast pyrolysis bio-oil (FPBO) and then upgraded via catalytic hydro-treatment at high pressure. Specifically, biomass feedstock goes through thermal cracking in the temperature range of 450–500 °C (absent of oxygen), which yields approximately 60–75 wt% liquid. The upgrading process can be varied according to specific requirements and applications field for a drop-in fuel and the blend ratio. Therefore hydro-treatment conditions such as H₂ pressure, temperature, catalyst type, and residential time can be manipulated to control the fuel quality. The pyrolysis oil also benefits from the wide range of biomass streams (i.e., inedible agricultural side products, roadside grass, and wood residues) [30]. The HPO is mixed with MGO in three mass ratios: 10%, 30%, and 50%, named: 10HPO, 30HPO, and 50HPO. Fig. 2 shows the samples of HPO blends. It can be seen that the liquid stays crystal clear and gets dark red at a high 50 wt% blend ratio. No phase separation was found after 2 months of still storage. The pure MGO and diesel (contains 7% bio-component, noted as B7) are also tested with the same operating conditions to serve as the reference. The viscosity and lubricity properties of HPO/MGO blends are also tested with Anton Paar Rheometer, as is listed in Table 2. A detailed description of the equipment and test method can be found in [31].

2.3. Test procedures

Before the test, the engine is warmed up at 800 rpm to keep the temperature of cooling water/oil above 75 °C. During the measurements, the engine is mainly running at 1200 rpm and 1425 rpm, which are the most typical cruise speeds and are referred to as A speed and B speed in the European stationary test cycle (ESTC). Three load conditions from low to high are gradually increased and tested at the A speed, while low and medium loads were chosen at the B speed, named A30/A50/A70 and B30/B50. The number refers to the percentage of the maximum load for the base engine at the respective speeds. Each measurement consists of 200 cycles, and the cylinder pressure signal is sampled and recorded for each of the cycles. Meanwhile, slow data, like inlet/exhaust, cooling oil/temperature information, and engine-out emissions are also recorded.

The investigation starts with benchmarking the HPO fuel blends with commercial fossil fuels (MGO and B7) on the HD diesel engine at the standard calibration with factory settings. These tests were carried out at 5 selected load/speed combinations which are assumed to be representative highway cruise operating loads. Then a charge preparation parameter study with variations of EGR rates and inlet temperatures at A30 is performed. The EGR is varied from 10% to 40% in steps of 10% and inlet temperature is changed from 35 $^{\circ}\mathrm{C}$ to 65 $^{\circ}\mathrm{C}$ in steps of 10 $^{\circ}\mathrm{C}$ while the other parameters are kept constant. Details of the operating conditions are shown in Table 3.

2.4. Data processing

All the measurements (200 cycles) are repeated 5 times and show good consistency and repeatability. The presented results are the averaged value of these repetitions and error bars are added to the figures. The net indicated mean effective pressure (nIMEP) is calculated from incylinder pressure over the four strokes of a full engine cycle (from -360 to $360\,^{\rm o}$ CA) based on Eq. (2), where P is the cylinder pressure, V_d is the displacement of test cylinder. The net indicated efficiency is based on Eq. (3), where $m_{\rm fuel}$ and LHV $_{\rm fuel}$ are fuel mass flow in each cycle and the lower heating value. Combustion efficiency is calculated based on the incomplete combustion products through Eq. (4), where IS_x and ISFC are the indicated specific emissions and indicated specific fuel consumption respectively. The recorded 200-cycle pressure date is first averaged and filtered. The specific filter is a combination of a 4-point moving average filter and a 10th-order low-pass filter with a cutoff frequency of 2500 Hz.

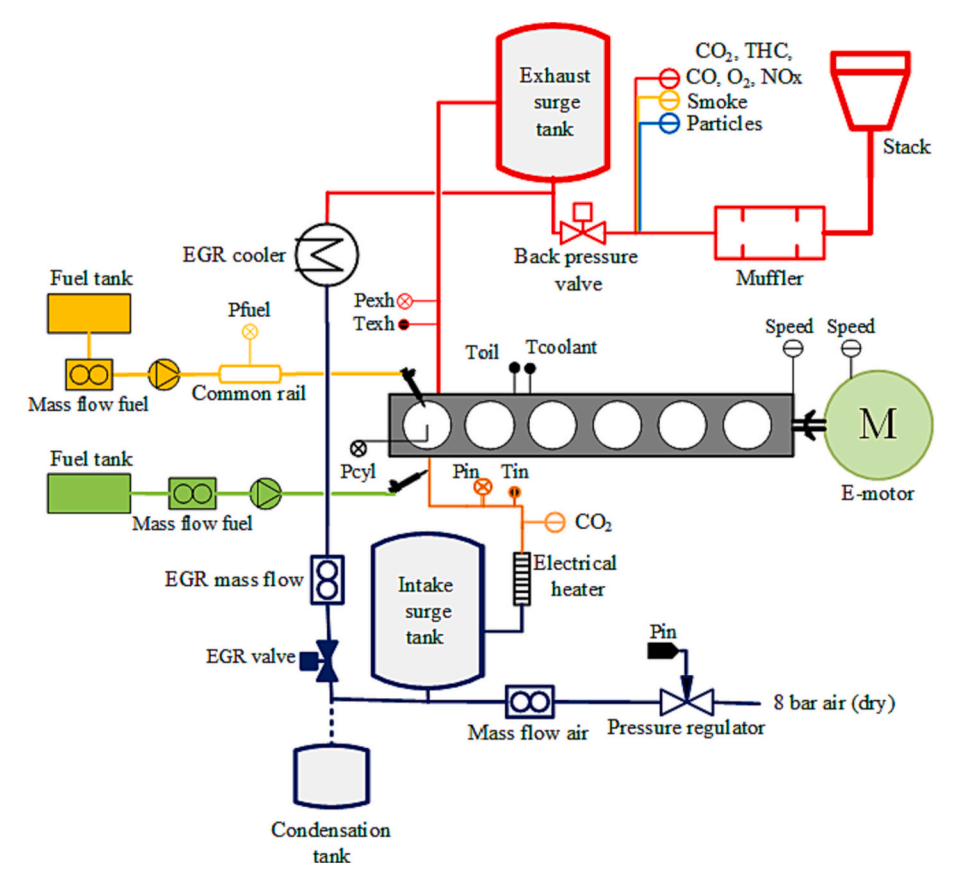


Fig. 1. Schematics of engine setup.



Fig. 2. Tested fuel samples.

Table 2Measured properties of HPO fuel blends.

Fuel	T [°C]	Viscosity [cP]	Total friction test [kJ]	$\begin{array}{c} \text{Total friction} \\ \text{average} \pm \text{SD} \\ \text{[kJ]} \end{array}$	Wear-scar [mm]
Diesel	25	3.13	1.12	1.055 ± 0.0675	0.55
10HPO	25	3.13	4.42	4.42	0.56
30HPO	25	3.11	3.37	3.37	0.34
50HPO	25	3.10	2.64	2.64	0.19

Table 3 Operating parameters.

	Unit	A30	A50	A70	B30	B50
Load	[%]	30	50	70	30	50
Speed	rpm	1200	1200	1200	1425	1425
EGR	[%]	26.1	24.1	23	26	28
Inlet pressure	[bar]	1.61	2.3	2.83	1.63	2.42
Back pressure	[bar]	1.77	2.67	3.16	1.92	2.75
Injection	[°CA aTDC]	-5.8	-4.5	-4.3	-8.8	-11.2
Fuel Pressure	[bar]	1557	1904	1931	1644	1735

The rate of heat release (ROHR) is calculated by Eq. (5) where θ is the crank angle and γ is the specific heat ratio. γ is determined by using the NASA polynomials and the average gas composition at each crank angle. The start of combustion (SOC) and end of combustion (EOC) is defined as the crank angle timing that 10% and 90% are released. Consequently, the ID and burn duration (BD) are the time intervals between SOI and SOC for ID (ID = SOC – SOI) and SOC and EOC (BD = EOC-SOC) respectively.

$$PM_{mass} = 4.95/0.405 \times FSN \times e^{0.38 \times FSN}$$
 (1)

$$gIMEP = \frac{\int\limits_{-360}^{360} P \times dV}{V_d} \tag{2}$$

$$\eta_{NIE} = \int_{-360}^{360} P \cdot dV / \left(m_{fuel} \cdot LHV_{fuel} \right) \times 100\%$$
 (3)

$$\eta_{combustion} = \left(1 - \frac{ISHC \cdot LHV_{fuel} + ISCO \cdot LHV_{CO} + ISH_2 \cdot LHV_{H_2}}{ISFC \cdot LHV_{fuel}}\right) \times 100\%$$
 (4)

$$ROHR = \frac{\gamma}{\gamma - 1} P \frac{\partial V}{\partial \theta} + \frac{1}{\gamma - 1} V \frac{\partial p}{\partial \theta}$$
 (5)

3. CRU results

Fig. 3 displays the ignition delay of tested fuels at various chamber pressure and EGR rate. Apparently, the ignition delay increases remarkably at a high EGR rate regardless of the chamber pressure. And it tends to decrease as the chamber pressure increases. The HPO blend ratio seems to have some influences in elongating the ignition delay at all CRU conditions, indicating a less reactivity of HPO compared to MGO and diesel. Specifically, it is noted that the ignition delay of all fuels at 50 bar is shorter than EOI (1 ms). As the chamber pressure decreases to 40 bar, 30HPO and 50HPO start to show some overlap with EOI at 40 and 30% EGR rates. At 30 bar, all fuels show overlap with EOI, and 50HPO is barely separated from EOI even without EGR, long fuel and air mixing time is expected. And the ignition delay time increases further at high EGR rate (nitrogen), due to less oxygen availability. The presented results show that the overall reactivity of the mixture depends both on property of fuel and ambient conditions.

The change in burn duration varies and depends both on the fuel and ambient conditions. As is shown in Fig. 4, the burn duration of diesel keeps increasing regardless of the chamber pressure. While the HPO/MGO blends show the same trend at 40 and 50 bar cases. As the chamber

pressure decreases to 30 bar, burn duration starts to decrease at a high EGR rate. To explain the change in burn duration, Fig. 5 illustrated the combustion process of 50HPO at various chamber pressure and EGR rates. Though the PRR profiles of all cases show a retarded and higher premixed combustion peak. Differences are shown among different chamber pressure cases. At 30 bar (Fig. 5a), the combustion profile (PRR) is featured with a premixed-dominant burn and small burn-out period. It is noticed that the premixed burn increases and after-burn decreases at high EGR rates, resulting a faster heat release. At 40 bar (Fig. 5b), combustion starts to overlap with injection events. EGR extends the ignition delay and plays a more crucial role in reshaping the combustion profiles. It can be seen that both premixed-dominant burn and after-burn period increase at a high EGR rate. The combined effects lead to the burn duration of 50HPO staying at a similar level as the EGR increases. As the chamber pressure increases further to 50 bar (Fig. 5c), a clear transition from mixing controlled to premixed dominant mode is shown. Yet, the after-burn period becomes more significant at the same time, which explains the increased burn duration time at a high EGR rate at 50 bar. The delayed combustion phasing is also validated on the chamber pressure curves. It can be seen that the pressure after combustion shifts towards the right direction at a high EGR rate regardless of the chamber pressures. Although it is reported in [32] that burn duration of mainly diffusive combustion decrease with ignition delay while burn duration of mainly premixed combustion increases with ignition delay. It has to be pointed out that increasing EGR (nitrogen percentage) decreases the global lambda, which shows noticeable impact on premixeddominant burn and after-burn period in the combustion process.

4. HPO fuel blends benchmarking

The results of engine benchmarking tests under a moderate EGR rate will be discussed in this section. It can be seen from Fig. 6 that all tested fuels show a similar combustion process in the engine from A30 to A70. The B7 and MGO fuels present a typical diesel heat-release shape: a minor premixed combustion period due to a short ignition delay followed by a large fraction of mixing-controlled combustion. For the cases with the HPO fuel blends, slightly retarded and (consequently) higher premixed combustion peaks are noticed, which is similar to the results from CRU due to less reactivity of HPO. The overall combustion progress and phasing are hardly affected though. Both cylinder pressure and the shape of the ROHR profiles are very close to those of B7 and MGO. As the load increases to A50 and A70, the aforementioned marginal differences of premixed peak among tested fuels becomes even more negligible. This is to be expected owing to both cylinder pressure and temperature increase at a high load and the reactivity difference plays a less important role. Furthermore, the fraction of premixed combustion decreases as the load increases regardless of the fuel type simply due to the fact that more fuel is injected automatically leading to an increase in the mixing-

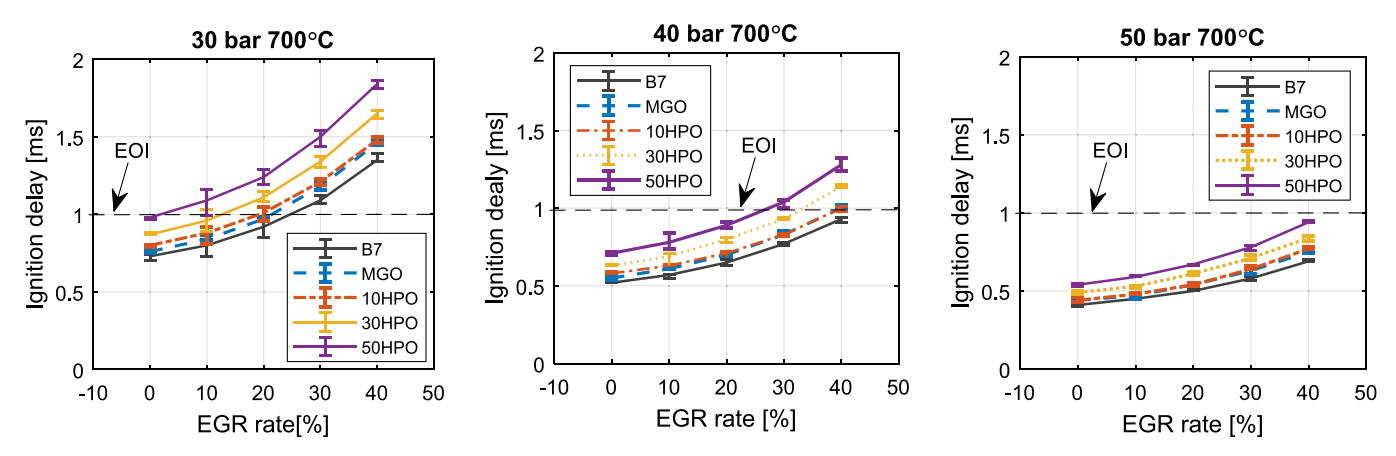


Fig. 3. Ignition delay of tested fuels at different chamber pressure and EGR rates.

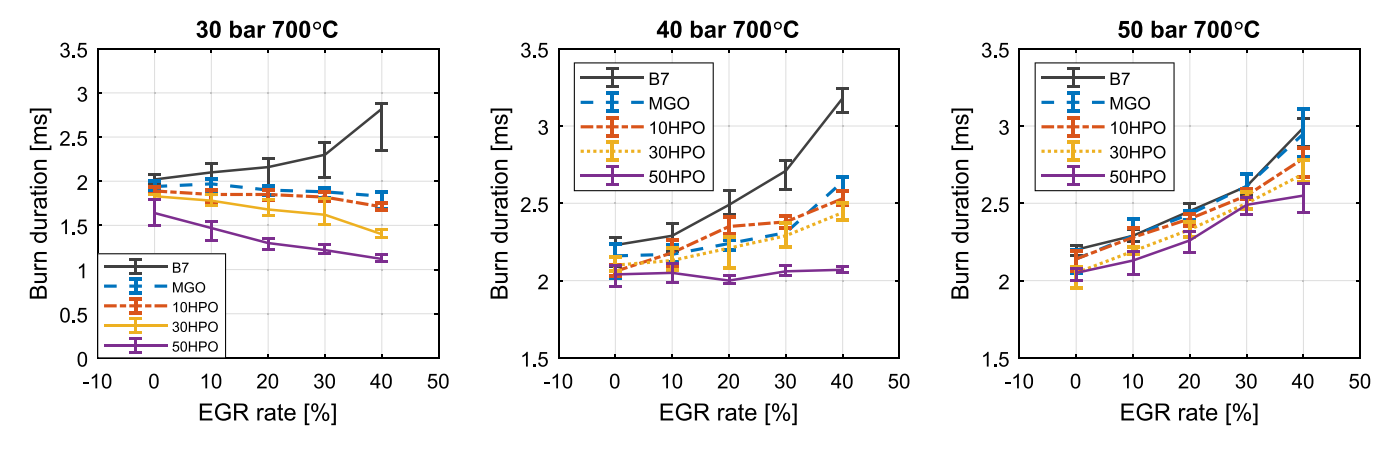


Fig. 4. Burn duration of tested fuels at various chamber pressure and EGR rates.

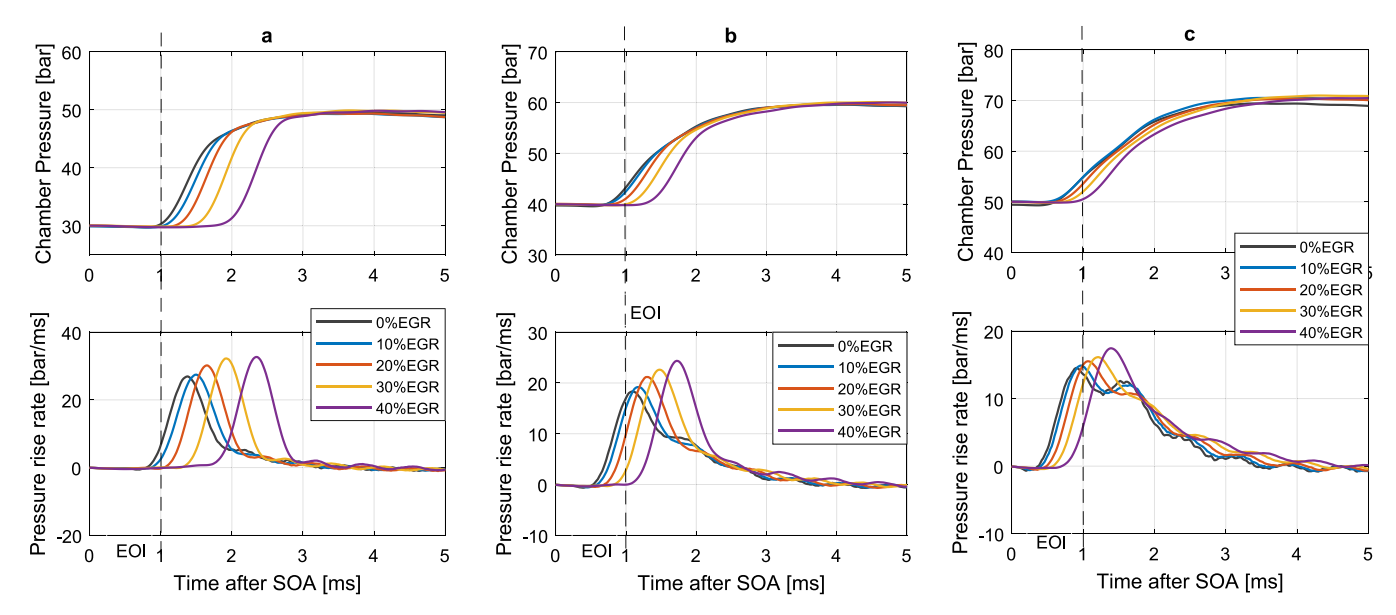


Fig. 5. Combustion process comparison of 50HPO of various EGR rates at 30 bar (a), 40 bar (b), 50 bar (c).

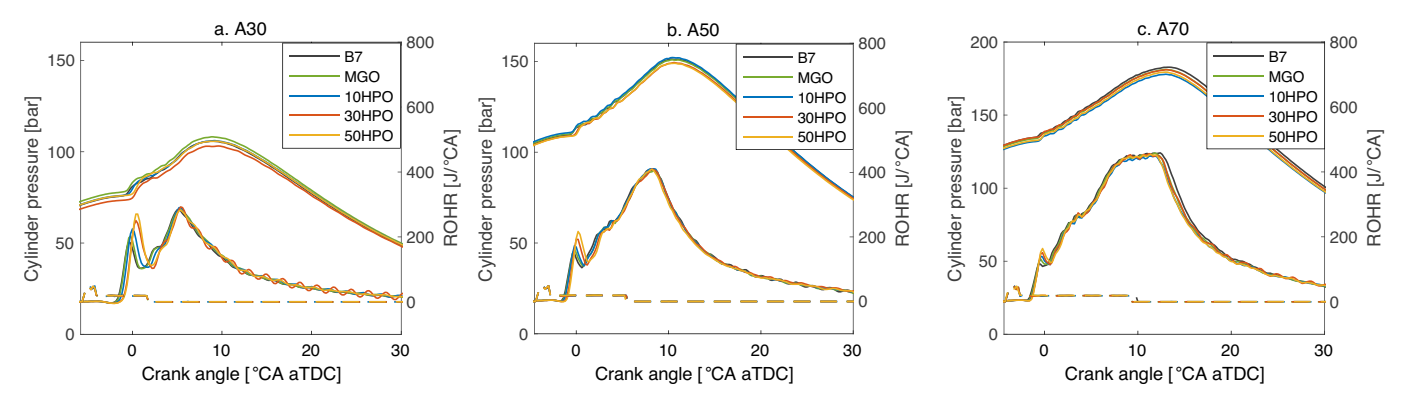


Fig. 6. Cylinder pressure and ROHR of tested fuels at A speed loads(Dashed line indicates injector current).

controlled phase.

To further illustrate the combustion process of HPO fuel blends, characteristic crank angles are plotted against the percentage of heat released in Fig. 7. Clearly, all fuels present the same start of combustion (CA10) and combustion phasing (CA50) including 50HPO. The only noticeable difference among tested fuels occurs for CA2 and CA90, where HPO fuel blends are slightly more retarded than MGO and B7.

Yet, these differences are just too small to affect engine operation. The combustion process and heat release timing at the B speed are plotted in Fig. 8 and Fig. 9. The differences are even smaller at the B speed. The presented results indicate the superior traits of HPO as drop-in fuels. It is safe to conclude base engine can just be operated with its base calibration when fueled with HPO blends.

The comparison of engine-out emissions of tested fuels at A speed/

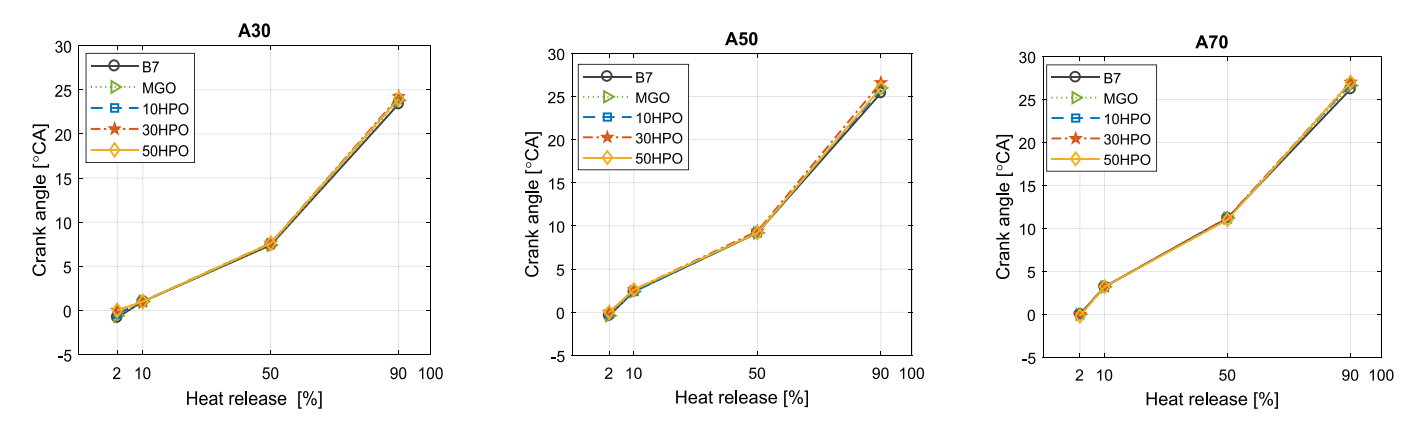


Fig. 7. Combustion phasing of tested fuels from A30 to A70.

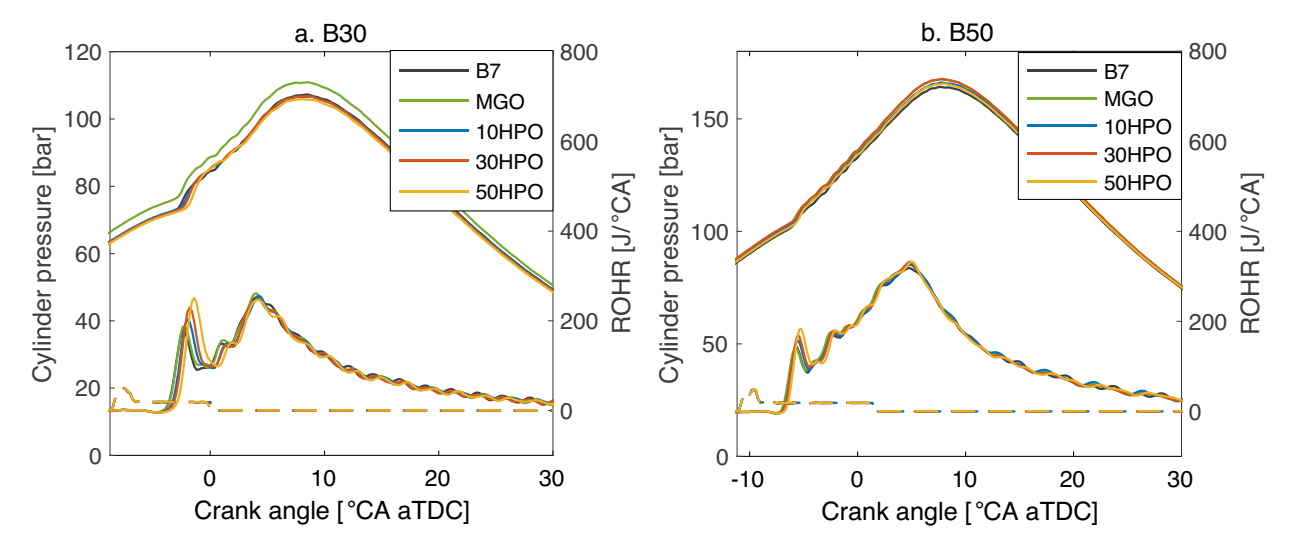


Fig. 8. Cylinder pressure and ROHR of tested fuels at B speed load points(Dashed line indicates injector current).

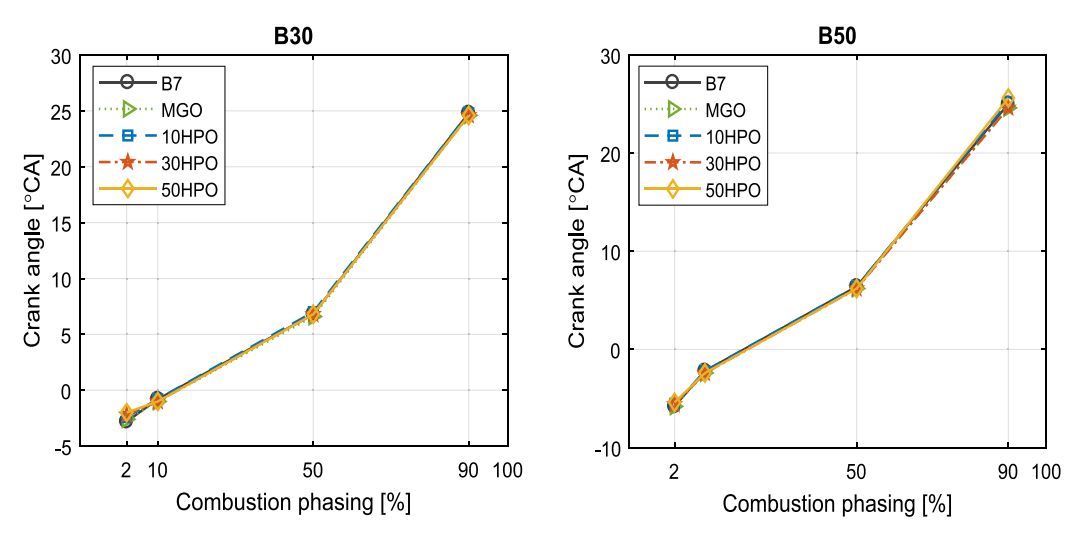


Fig. 9. Combustion phasing of tested fuels at B30 and B50.

loads is shown in Fig. 10. It can be seen that both CO and unburnt HC emissions decrease as the load increases. This is not just caused by increased ambient temperature and pressure which promotes a completed combustion process. The more retarded injection timings at high loads also reduce the fuel spray trapped in the crevice volume, leading to lower unburnt HC emissions. In addition, the increased inlet

temperature and pressure at high loads also contribute to improved overall oxidation. The NOx emissions present a general increasing trend as the load increases. This is assumed to be due to the increase in local combustion temperature at higher loads. Interestingly, it can be noticed that HPO fuel blends yield lower NOx emissions than MGO. Note that the base calibration produces extremely low engine-out ISPM emissions

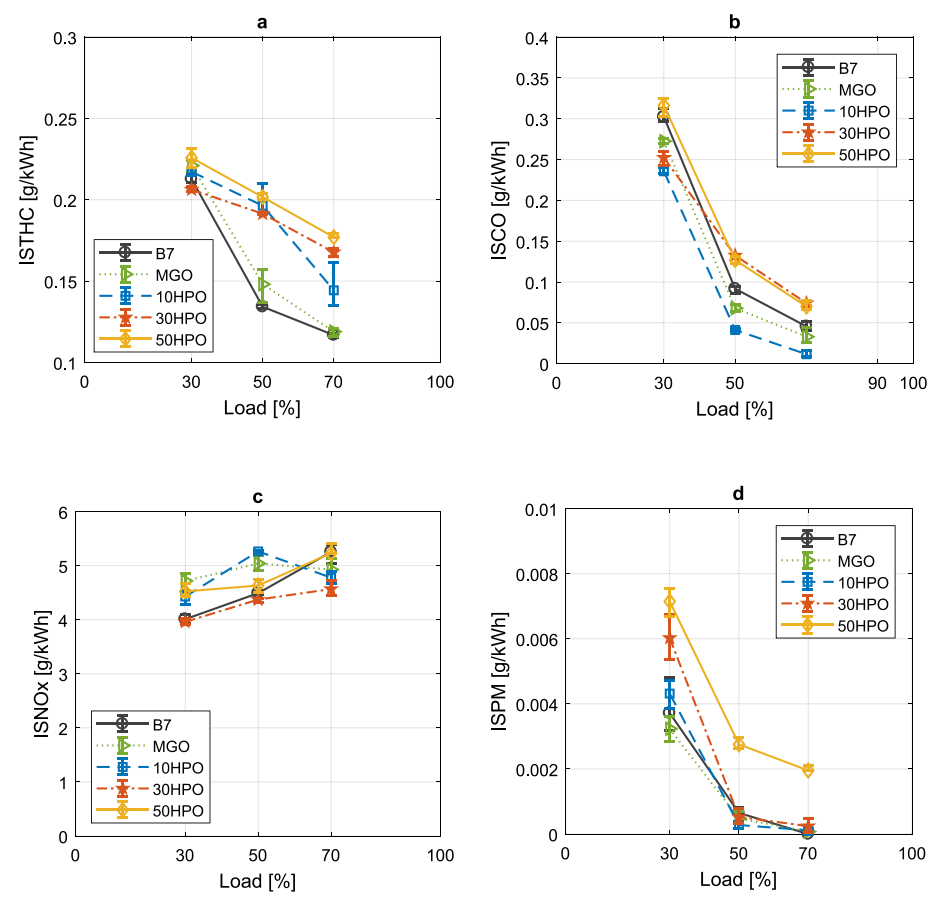


Fig. 10. Engine-out emissions of tested fuels at A speed loads.

from A30 to A70, well below the Euro VI standard (0.01 g/kWh) for all fuels, and decreases even further at high load conditions. The NOx emissions on the other hand, generally increases at high load. And the typical NOx-soot tradeoff is observed as the increases of operating loads. This could be explained by the increased combustion temperature at high loads, which promotes the formation of thermal NOx and oxidation of soot emissions. It is also noticed that the PM emissions of HPO blends are higher than MGO and B7 and increase with the blend ratio. This might be related to the composition of HPO fuels. The aromatic components in the fuel might be the cause for the higher PM. Still, the overall engine-out emissions are too low to be of concern. In general, the HPO

blends show attractive emissions traits: less NOx, minor increases in HC/PM, and a similar level of CO emissions compared to B7 and MGO.

The efficiencies are shown in Fig. 11. All fuels yield the typical high combustion efficiency for compression ignition engines, close to 100% combustion. It increases further as the load increases. The addition of HPO barely makes any difference in combustion efficiency. The net indicated efficiency (NIE), is above 45% regardless of the operating load and fuel types. NIE decreases marginally as the HPO blends increase. It is minimal at 50 wt% of HPO in the blend but still only a 1% decrease compared to pure MGO.

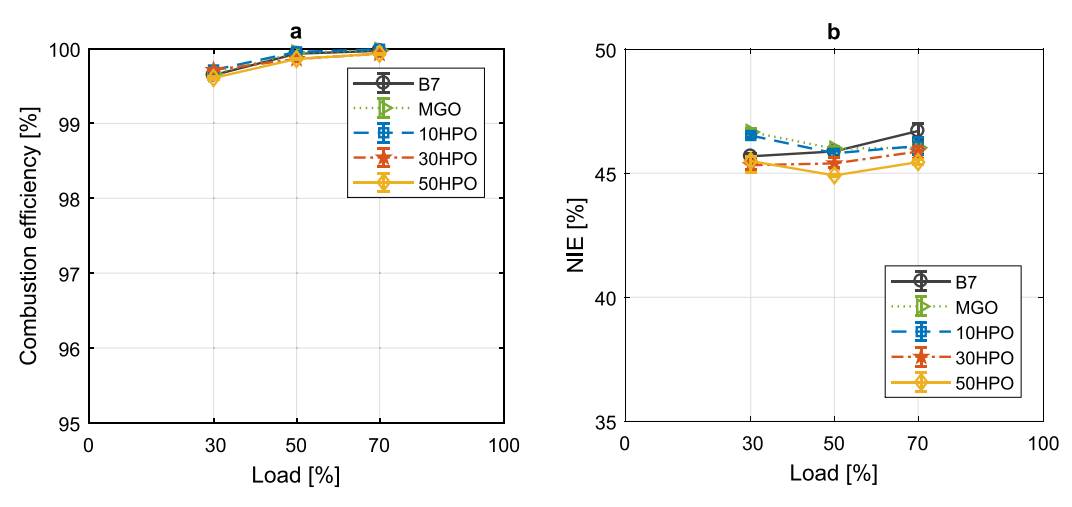


Fig. 11. Combustion efficiency and net indicated efficiency.

5. Effects of EGR

The results of EGR variation will be discussed in this section. The effects of EGR on the combustion process of HPO blends are illustrated in Fig. 12. As is expected, the EGR effectively extends the ignition delay time for all fuels (Fig. 13a). It is shown that all ROHR profiles shift to the right illustrating the increasing delay with increasing EGR rate. It is worth noting a minor increase in the premixed combustion peak among the tested fuels at high EGR rates. This is mainly related to the longer ignition time so that a larger portion of the fuel/air mixture gets better premixed. Similarly, less mixing-controlled combustion is expected, which is verified by the decreasing second ROHR peak as the EGR rate increases. Furthermore, the overall delayed combustion phasing also contributes to a lower cylinder pressure peak for the high EGR cases, regardless of the fuel type. Meanwhile, the increased heat capacity due to reduced exhaust gas also decreased the bulk combustion temperature and therefore slower overall heat release process. Therefore, an extended burn duration is shown in Fig. 13b as the EGR rate increases for all fuels. The differences in BD among the tested fuels, however, are negligible.

The regulated engine-out emissions at various EGR rates are shown in Fig. 14. The unburned HC emissions of B7, MGO, and 10HPO decrease at a high EGR rate while HC emissions of 30HPO and 50HPO first decrease to 30% EGR rate and then increases remarkably at 40% EGR again. This is assumed to be due to the longer injection duration for

higher blend ratios to keep the same engine load. Consequently, more fuel may be trapped in the crevice volume and suffers from incomplete combustion. CO emissions increase significantly as the EGR rate increases for all fuels. This is due to the decreased oxygen availability and lower temperature, which promotes local fuel-rich areas and deteriorates further oxidation from CO to CO₂ respectively. In addition, CO increases as the HPO blend ratio increases. The typical NOx-soot for CI engines trade-off is observed in Fig. 14c. All fuels yield a significant decrease in NOx emissions while PM emissions increase at a high EGR rate. At 40% EGR, all fuels including the HPO blends can achieve 1 g/ kWh ISNOx and 0.1 g/kWh ISPM (engine-out level). Again, the HPO blends show higher PM emissions compared to MGO and B7 and show a higher sensitivity with respect to the EGR rate. As is shown in Fig. 14c, 30HPO produces the highest PM emissions as the EGR value of 30HPO (41.2%) is somewhat higher than that of 10HPO (40%) and 50HPO (40.1%) cases.

Fig. 15 shows the efficiencies of tested fuels at various EGR rates. Both combustion efficiency and net indicated efficiency decrease at a high EGR rate for all fuels. However, the HPO blends do exhibit a lower value for the NIE for all cases. It is also observed that combustion efficiency and NIE decrease as the HPO blend ratio increases. Still, the 30HPO and 50HPO achieve 99.2% combustion efficiency and 45% net indicated efficiency at a 40% EGR rate.

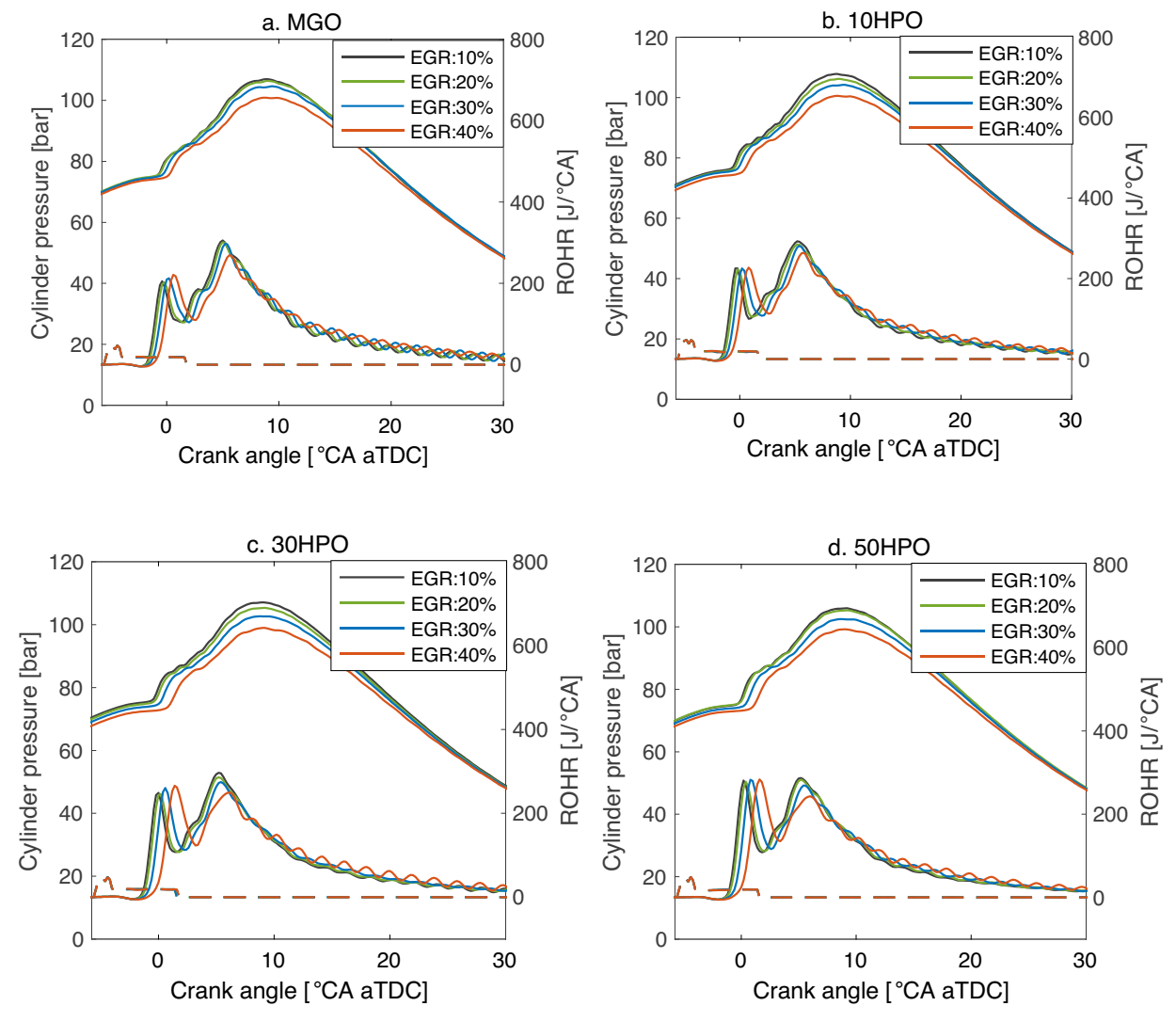


Fig. 12. Cylinder pressure and ROHR for HPO fuel blends at various RGR rates(Dashed line indicates injector current).

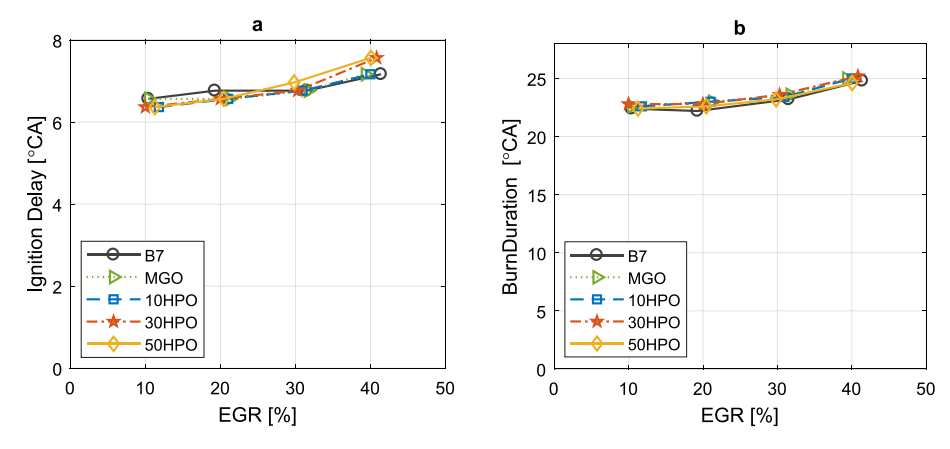


Fig. 13. Ignition delay and Burn duration as a function of the EGR rate of tested fuels.

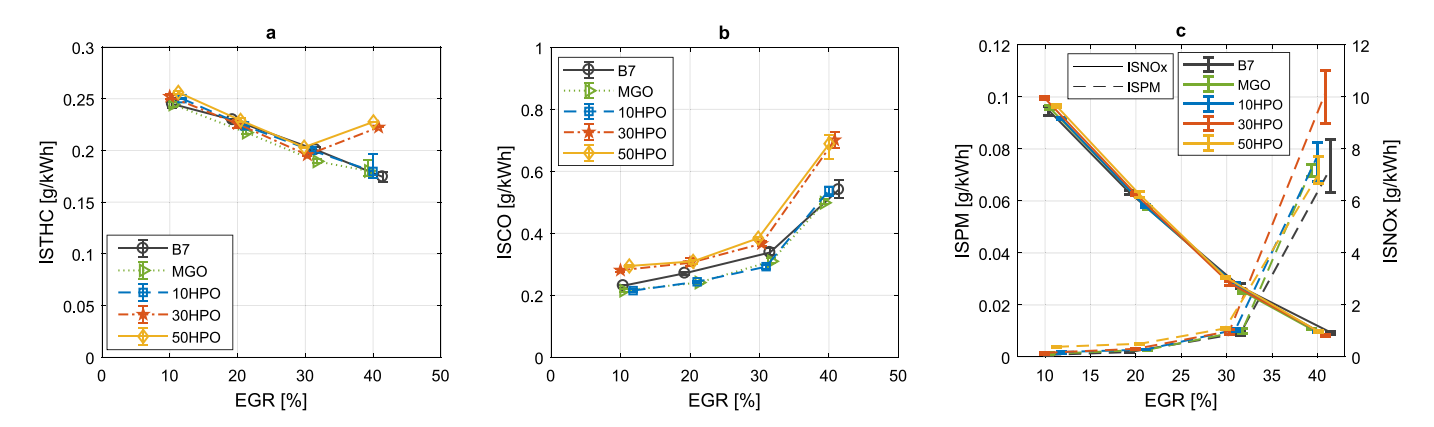


Fig. 14. Engine-out emissions as a function of EGR for tested fuels.

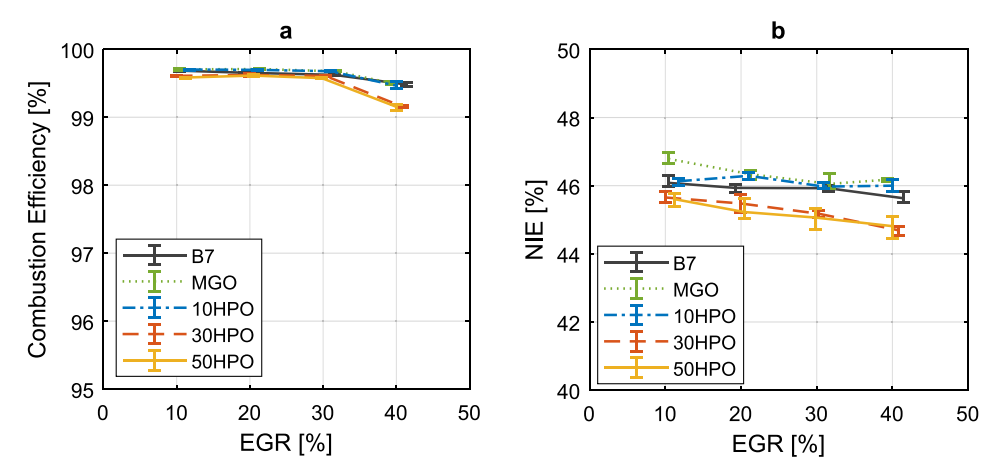


Fig. 15. Efficiencies of tested fuels as a function of EGR rate.

6. Effects of inlet temperature

The results of the inlet temperature sweep will be discussed in this section. As is shown in Fig. 16, the inlet temperature has a much lower impact on the combustion process of HPO blends than EGR. The higher inlet temperature is supposed to facilitate the auto-ignition of the fuel/air mixture. Therefore, inlet heating is commonly used at cold start and low load conditions to promote ignition for LTC concepts [33]. And it is observed that all fuels present a minor earlier and smaller premixed combustion peak. However, the temperature steps (10 $^{\circ}$ C) are too small to make a visible difference. The main mixing—controlled combustion

phasing seems to be identical for all cases. The ignition delay and burn duration are therefore expected to remain constant at these different temperature cases. It is necessary to point out that the differences in the cylinder pressure traces are due to the drift of the inlet pressure setting. To account for this uncertainty, the sequence in the test procedure is randomized.

Fig. 17 illustrates the effects of inlet temperature on regulated emissions. The CO and HC emissions are relatively constant for all the temperature cases regardless of the fuel type. PM emissions are kept at an extremely low level (0.003–0.008 g/kWh) and consistent with the previous sections. The PM emissions increase as the HPO blend ratio

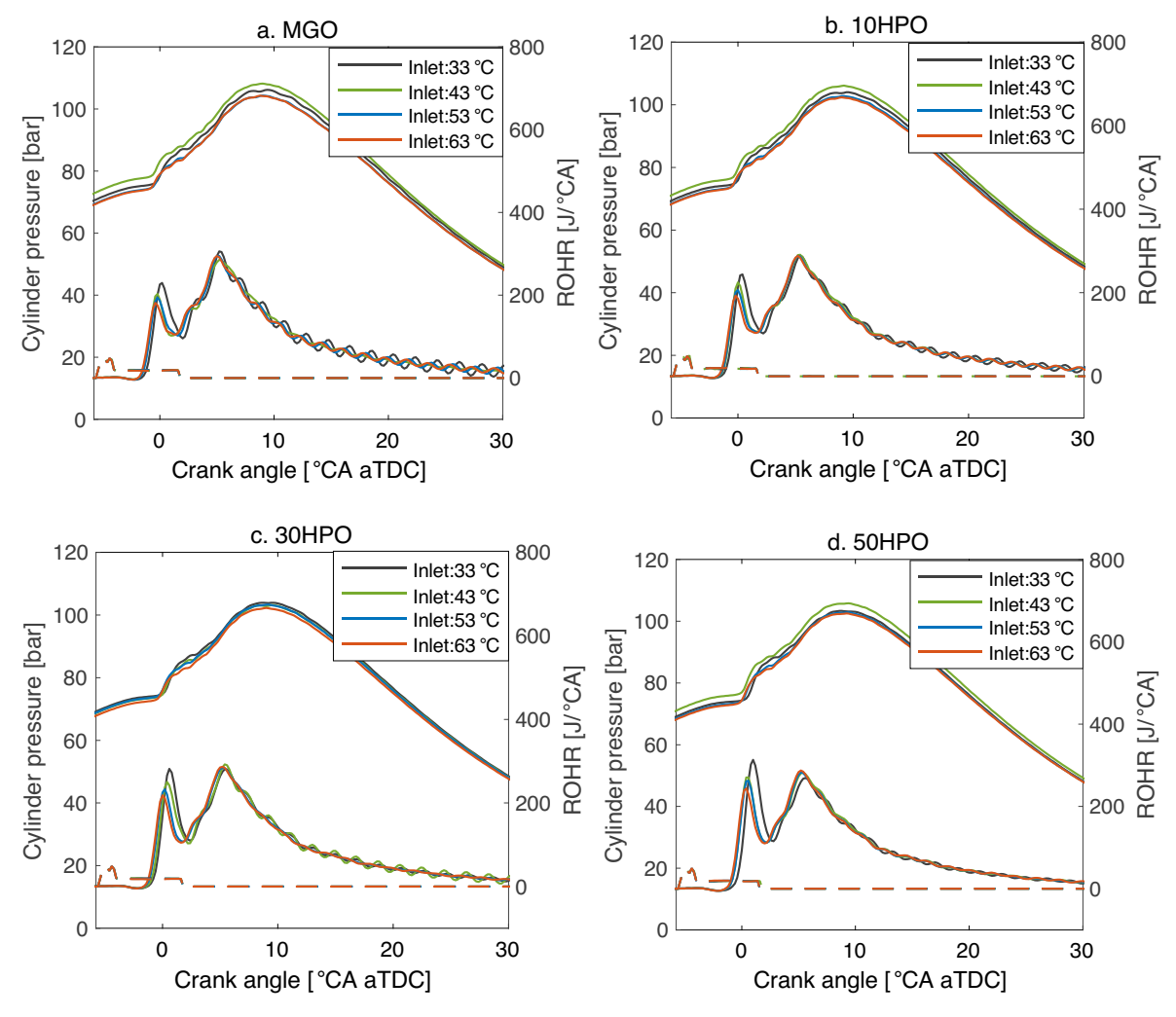


Fig. 16. Cylinder pressure and ROHR of tested fuels at various inlet temperatures(Dashed line indicates injector current).

increases. And a small increase in NOx emissions at high inlet temperatures is noticed for all fuels, possibly due to higher combustion temperatures. Especially, ISNOx of 30HPO increases from 4 g/kWh to 5 g/kWh. Among the HPO blends, the trend of NOx emissions does not show a good correlation with the blend ratios.

The combustion efficiency generally stays above 99.5% regardless of the inlet temperature for all fuels. Therefore, for fuels that have a similar reactivity with diesel under engine conditions, inlet heating barely shows any benefits in promoting combustion and oxidation. In addition, roughly a 1% reduction is shown on the net indicated efficiency, as is shown in Fig. 18. This can be explained by the change of inlet charge. The inlet density decreases as inlet temperature increases, which leads to less mass trapped in the cylinder, such that higher bulk combustion temperature and higher heat transfer loss can be expected [34]. In addition, simulation work [35] also the change of specific heat at high inlet temperature is the largest contributor to the decreased indicated efficiency.

7. Summary and conclusions

In this work, a second-generation biofuel, HPO is blended with MGO at various mass ratios. They are benchmarked with commercial fuels like MGO and diesel (B7) both on CRU and HD diesel engines with EGR. Following the engine tests with standard calibration settings, charge preparation parameter study is performed to investigate the effects of EGR rate and inlet temperature on HPO fuels. Based on the results, the

following conclusions can be made:

- Under CRU conditions, ignition delay increases with HPO blend ratio and EGR rates. HPO blends yield shorter burn duration regardless of the operating condition due to a better-premixed charge, therefore faster heat release.
- 2. Up to 50 wt% HPO can be blended and operated in an HD engine safely. Compared with MGO and diesel, HPO fuel blends present identical combustion behavior from low to high loads at the two tested speeds. Though HPO fuels yield a marginally higher premixed combustion peak and fraction, the influence of which is too small to be noticed in the application. As the load increases, the difference in ROHR shape is negligible, and key combustion phasing (CA10, CA50, and CA90) nearly overlaps for diesel, HPO/MGO fuel blends.
- 3. Under the default calibration, the engine-out ISPM emissions are kept at the set low level, regardless of the fuel type. Even though ISPM emissions increase slightly as the HPO blend ratio increases, the engine-out PM emissions are still well below the Euro VI norm. All fuels present relatively high ISNOx emissions (above 4 g/kWh) at this calibration, yet HPO addition decreases the engine-out ISNOx. HC/CO emissions of HPO blends tend to increase compared to MGO and B7.
- 4. Both combustion efficiency and net indicated efficiency increase as the load increases. Specifically, all fuels yield a combustion efficiency over 99.5% and a net indicated efficiency over 45%. The HPO

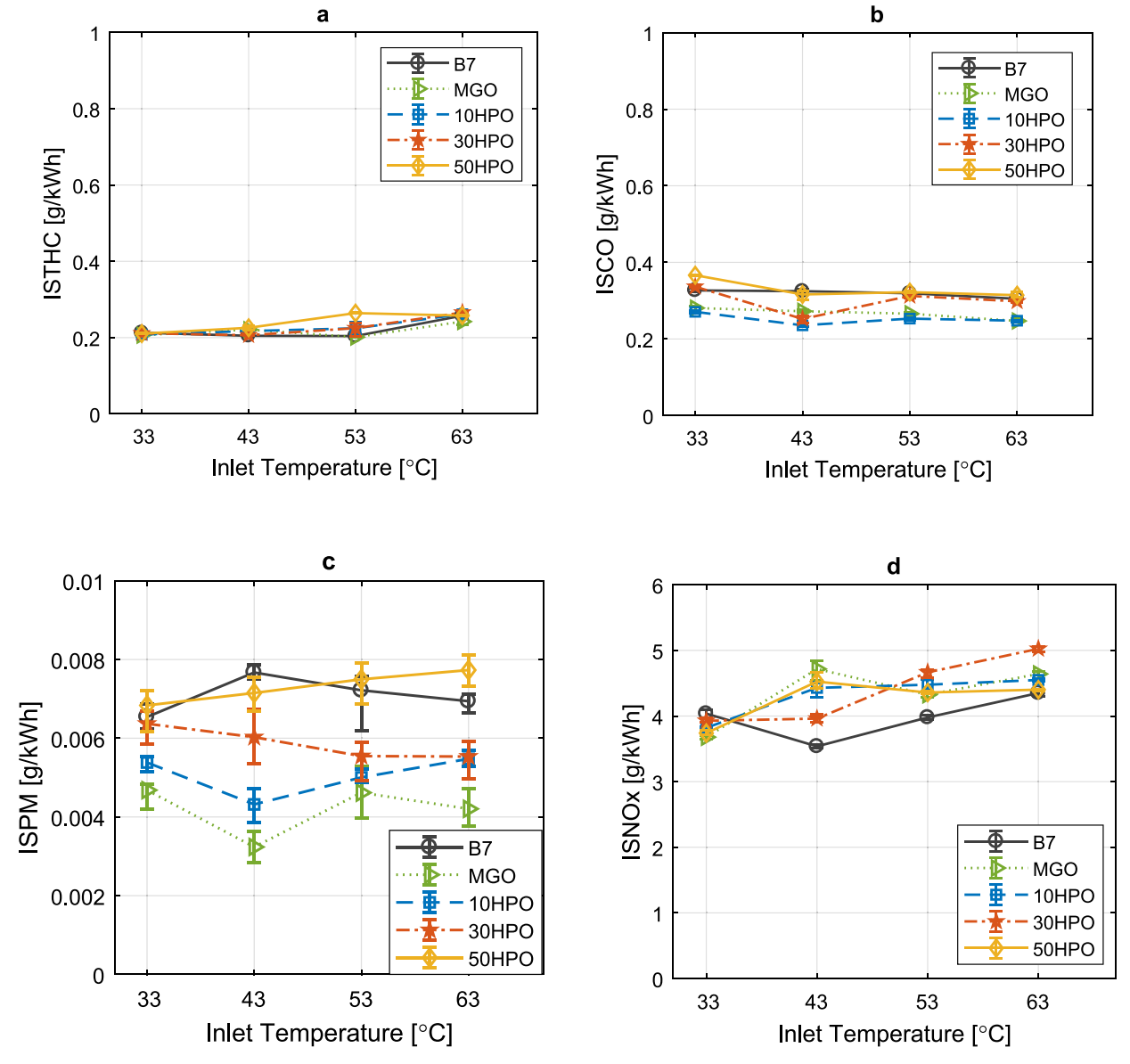


Fig. 17. Engine-out emissions as a function of Inlet temperature.

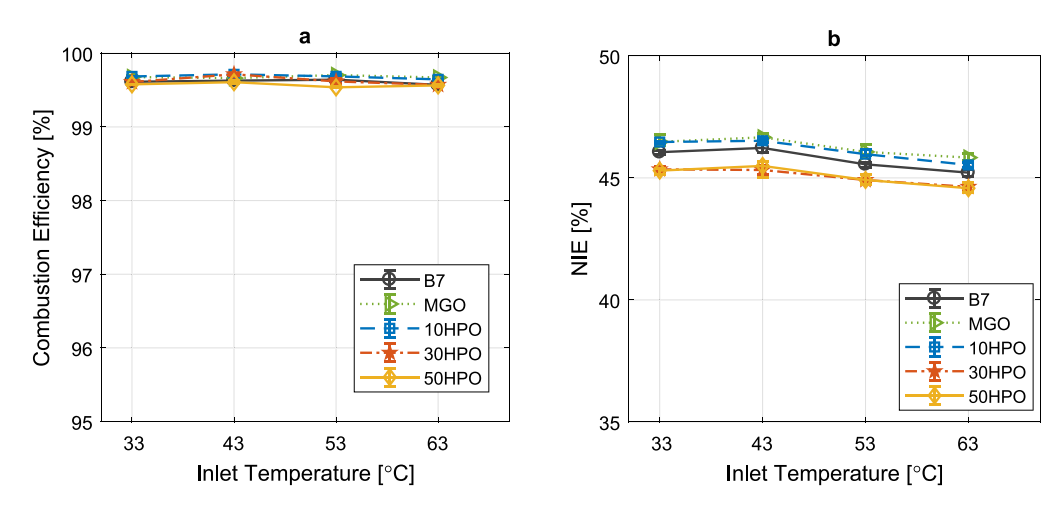


Fig. 18. Combustion efficiency and net indicated efficiency as a function of inlet temperature.

- blends systematically yield a slightly lower ($\sim 1\%$ for 50HPO) NIE compared to MGO and diesel.
- 5. As the EGR increases, all fuels present an increased ignition delay, and longer burn duration. As expected, the typical NOx/soot tradeoff relation holds for all fuels and about 1% decreased combustion/indicated efficiency is observed at a high EGR rate as expected when EGR increased from 10 to 40%. At 40% EGR, 1 g/kWh ISNOx is achieved whilst keeping the ISPM below 0.1 g/kWh. It is worth noticing though that PM emissions of HPO fuel blends are more sensitive to EGR than MGO and B7.
- 6. Due to the similar reactivity of HPO blends with commercial fuels, the inlet temperature barely shows any effects on the combustion. In addition, engine-out emissions remain comparable as inlet temperature increases. Inlet heating does decrease the net indicated efficiency by about 1%.

The presented promising performance and emission results indicate the viability of applying HPO in the existing infrastructure and its use in power generation devices. No major hardware modification and recalibration are required to fuel the engine with drop-in biofuels. Due to the limited fuel supply, the durability test cannot be conducted. It is the authors intention to carry out long consecutive time test on the engine setup to study the impact of HPO addition on fueling system (such as fuel pump, injectors) and oil contaminations and rubber parts of engine in future work. Though up to 50 wt% HPO ratio is applied, the higher blend ratio or even 100% HPO are worthwhile investigating. Particularly, when the base fuel is also bio-originated and commercially available such as HVO, a fully carbon-neutral fuel blend can be realized, allowing an easy-to-implement reduction in GHG emissions for the existing fleets.

CRediT authorship contribution statement

Jinlin Han: Writing – original draft, Methodology, Investigation, Formal analysis, Data curation. **L.M.T. Somers:** Writing – review & editing, Supervision, Resources, Project administration, Funding acquisition. **Bert van de Beld:** Writing – review & editing, Resources, Project administration, Funding acquisition, Conceptualization.

Declaration of competing interest

The authors declare that they have no known competing financial interests or personal relationships that could have appeared to influence the work reported in this paper.

Data availability

Data will be made available on request.

References

- [1] M. Storch, F. Hinrichsen, M. Wensing, S. Will, L. Zigan, The effect of ethanol blending on mixture formation, combustion and soot emission studied in an optical DISI engine, Appl. Energy 156 (2015) 783–792.
- [2] H. Huang, W. Teng, Q. Liu, C. Zhou, Q. Wang, X. Wang, Combustion performance and emission characteristics of a diesel engine under low-temperature combustion of pine oil-diesel blends, Energy Convers. Manag. 128 (2016) 317–326.
- [3] A.T. Hoang, A.I. Ölçer, S. Nižetić, Prospective review on the application of biofuel 2, 5-dimethylfuran to diesel engine, J. Energy Inst. 94 (2021) 360–386.
- [4] Q. Zhang, G. Chen, Z. Zheng, H. Liu, J. Xu, M. Yao, Combustion and emissions of 2, 5-dimethylfuran addition on a diesel engine with low temperature combustion, Fuel 103 (2013) 730–735.
- [5] H. Xiao, P. Zeng, L. Zhao, Z. Li, X. Fu, An experimental study of the combusition and emission performances of 2, 5-dimethylfuran diesel blends on a diesel engine, Therm. Sci. 21 (1 Part B) (2017) 543–553.
- [6] Q. Zhang, X. Hu, Z. Li, B. Liu, Z. Chen, J. Liu, Combustion and emission characteristics of diesel engines using diesel, DMF/diesel, and n-pentanol/diesel fuel blends, J. Energy Eng. 144 (3) (2018) 4018030.
- [7] Z. Zheng, X. Wang, X. Zhong, B. Hu, H. Liu, M. Yao, Experimental study on the combustion and emissions fueling biodiesel/n-butanol, biodiesel/ethanol and biodiesel/2, 5-dimethylfuran on a diesel engine, Energy 115 (2016) 539–549.

- [8] X. Li, Z. Xu, C. Guan, Z. Huang, Effect of injection timing on particle size distribution from a diesel engine, Fuel 134 (2014) 189–195.
- [9] M.A. Ghadikolaei, C.S. Cheung, K.F. Yung, Comparison between blended mode and fumigation mode on combustion, performance and emissions of a diesel engine fueled with ternary fuel (diesel-biodiesel-ethanol) based on engine speed, J. Energy Inst. 92 (5) (2019) 1233–1250.
- [10] J. Han, L.M.T. Somers, Comparative investigation of ignition behavior of butanol isomers using constant volume combustion chamber under diesel-engine like conditions, Fuel 304 (2021) 121347.
- [11] J. Han, S. Wang, R.M. Vittori, L.M.T. Somers, Experimental study of the combustion and emission characteristics of oxygenated fuels on a heavy-duty diesel engine, Fuel 268 (2020) 117219.
- [12] J. Han, Alcohol Applications in Heavy-Duty Diesel Engines, Technische Universiteit Eindhoven, 2020.
- [13] J. Han, Y. Wang, B. Somers, 2021, Experimental Investigation of Viscosity and Combustion Characteristics of N-Butanol/Diesel Blends, SAE Technical Papers, 2021
- [14] J. Han, W. He, L.M.T. Somers, Experimental investigation of performance and emissions of ethanol and n-butanol fuel blends in a heavy-duty diesel engine, Front. Mech. Eng. 6 (2020) 26.
- [15] J. Han, S. Wang, L.M.T. Somers, 2018, Effects of different injection strategies and EGR on partially premixed combustion, SAE Technical Papers, 2018.
- [16] J. Han, L.M.T. Somers, R. Cracknell, A. Joedicke, R. Wardle, V.R.R. Mohan, Experimental investigation of ethanol/diesel dual-fuel combustion in a heavy-duty diesel engine, Fuel 275 (2020) 117867.
- [17] J. Han, H. Bao, L.M.T. Somers, Experimental investigation of reactivity controlled compression ignition with n-butanol/n-heptane in a heavy-duty diesel engine, Appl. Energy 282 (2021) 116164.
- [18] J. Han, B. Somers, Effects of Butanol Isomers on the Combustion and Emission Characteristics of a Heavy-Duty Engine in RCCI Mode (No. 2020-01-0307), SAE Technical Paper, 2020.
- [19] M. Okcu, M. Fırat, Y. Varol, Ş. Altun, F. Kamışlı, O. Atila, Combustion of high carbon (C7-C8) alcohol fuels in a reactivity controlled compression ignition (RCCI) engine as low reactivity fuels and ANN approach to predict RCCI emissions, Fuel 319 (2022) 123735.
- [20] M.K. Yesilyurt, A detailed investigation on the performance, combustion, and exhaust emission characteristics of a diesel engine running on the blend of diesel fuel, biodiesel and 1-heptanol (C7 alcohol) as a next-generation higher alcohol, Fuel 275 (2020) 117893.
- [21] M. Zubel, S. Pischinger, B. Heuser, Assessment of the full thermodynamic potential of C8-oxygenates for clean diesel combustion, SAE Int. J. Fuels Lubricant. 10 (3) (2017) 913–923.
- [22] K. Munch, T. Zhang, A Comparison of Drop-in Diesel Fuel Blends Containing Heavy Alcohols Considering both Engine Properties and Global Warming Potentials (No. 2016-01-2254), SAE Technical Paper, 2016.
- [23] T. Zhang, K. Munch, I. Denbratt, An experimental study on the use of butanol or octanol blends in a heavy duty diesel engine, SAE Int. Journal of Fuels and Lubricants 8 (3) (2015) 610–621.
- [24] M. Zubel, O.P. Bhardwaj, B. Heuser, B. Holderbaum, S. Doerr, J. Nuottimäki, Advanced fuel formulation approach using blends of paraffinic and oxygenated biofuels: analysis of emission reduction potential in a high efficiency diesel combustion system, SAE Int. Journal of Fuels and Lubricants 9 (3) (2016) 481–492.
- [25] M. Zubel, S. Pischinger, B. Heuser, Assessment of the full thermodynamic potential of C8-oxygenates for clean diesel combustion, SAE Int. Journal of Fuels and Lubricants 10 (3) (2017) 913–923.
- [26] B.E.N.E.D.I.K.T. Heuser, M. Jakob, F. Kremer, S. Pischinger, B. Kerschgens, H. Pitsch, Tailor-made fuels from biomass, in: Influence of Molecular Structures on the Exhaust Gas Emissions of Compression Ignition Engines (no. 2013-36-0571), SAE Technical Paper, 2013.
- [27] J. Han, Y. Wang, L.M.T. Somers, B. van de Beld, Ignition and combustion characteristics of hydrotreated pyrolysis oil in a combustion research unit, Fuel 316 (2022) 123419.
- [28] W.F. Northrop, S.V. Bohac, J.Y. Chin, D.N. Assanis, Comparison of Filter Smoke Number and Elemental Carbon Mass from Partially Premixed Low Temperature Combustion in a Direct-Injection Diesel Engine, 2011.
- [29] https://www.btgworld.com/en.
- [30] J. Han, L.M.T. Somers, B. van de Beld, Combustion and emission characteristics of hydrotreated pyrolysis oil on a heavy-duty engine, Fuel 351 (2023) 128888.
- [31] J. Han, Y. Wang, B. Somers, Experimental Investigation of Viscosity and Combustion Characteristics of N-Butanol/Diesel Blends (No. 2021-01-0555), SAE Technical Paper, 2021.
- [32] S. Rabl, T.J. Davies, A.P. McDougall, R.F. Cracknell, Understanding the relationship between ignition delay and burn duration in a constant volume vessel at diesel engine conditions, Proc. Combust. Inst. 35 (3) (2015) 2967–2974.
- [33] J. Han, S. Wang, B. Somers, Comparative study on the effects of inlet heating, inlet boosting, and double-injection strategy on partially premixed combustion, in: SAE Technical Papers 2019, 2019.
- [34] S. Wang, P.C. Bakker, L.M.T. Somers, L.P.H. de Goey, Effect of air-excess on blends of RON70 partially premixed combustion, Flow, Turbulen. Combustion 96 (2) (2016) 309–326.
- [35] N. Lam, P. Tunestal, A. Andersson, Analyzing Factors Affecting Gross Indicated Efficiency when Inlet Temperature Is Changed (No. 2018-01-1780), SAE Technical Paper, 2018.